

Effect of threading on static and dynamic properties of polymer chains in entangled linear-ring blend systems with different stiffness

Wei Wang^a, Jibao Lu^{a,b,*}, Rong Sun^{a,b}

^a Shenzhen Institute of Advanced Electronic Materials, Chinese Academy of Sciences, Shenzhen, 518055, China

^b Shenzhen Institute of Advanced Technology, Chinese Academy of Sciences, Shenzhen, 518055, China

ABSTRACT

Threading is a unique topological state in linear/ring polymer blends (LRB), which is considered to be essential for evaluating both the static and dynamic properties of ring polymer (RP)-containing polymer melts. In the present work, we use molecular dynamics simulations with the Kremer-Grest model to systematically investigate the threading event and its effect on the properties of RP in linear polymer (LP) dominated LRB. The chain stiffness is also considered in the simulation to represent a wider range of polymer systems. To obtain the exact number of threads for each RP chain, the inner minimal surface (IMS) technique is applied. We find that for a wide range of chain lengths, the number of threads can be roughly estimated using the predetermined entanglement number for RP chains with different stiffness. The number of threads follows a Gaussian distribution, and the width increases monotonically for longer and stiffer chains. The effect of threading on both the size and shape of RP chains is investigated. We find that for RP chains of different chain lengths, the effect of threading on polymer size is more pronounced for more flexible chains. The effect of threading on shape of RP is also enhanced for longer chains, but the sensitivity of the shape to threading is indistinguishable for RP chains of different stiffness. The dynamics of threading is also studied in this work, and a much slower relaxation time is found for more flexible chains. In conclusion, we have developed a method that can directly detect the threading events in LRB, which allows us to quantitatively study the effect of threading. The result obtained by this method is also expected to be integrated into the viscoelastic theory to better estimate the rheological properties of LRB systems.

1. Introduction

Over the last few decades, ring polymers (RPs) have been extensively studied, but how the topology affects the static and dynamic properties of the melt system, especially when blended with linear polymers (LPs), remains to be elucidated [1–22]. The linear/ring polymer blend (LRB) is a topological polymer blend with many unique properties that differ from the pure LP or RP melts. One major difference is the special topological state: threading. Although threading between different chains is rare in pure RP melts, especially for those with relatively short chain lengths [23], RP chains are often found to be threaded by the LP chains in LRB due to the entropy favorability demonstrated in both experiments and simulations, especially when the fraction of LP chains is dominant [24].

As a topological constraint besides entanglement, threading significantly affects the rheological properties of the LRB systems [25–28]. For example, the linear viscoelastic response of the RP melts decreases drastically if LP contaminant is not completely removed during the purification process [29,30]. Meanwhile, mixing a small amount of entangled RPs into LP matrix significantly reduces the RP diffusivity [25] and increases the viscosity of the whole system [30], as LP chains

tend to penetrate into the interior of the RPs with a more expanded configuration. In pure LP melts, the chains can relax through the typical reptation mechanism. However, in LRBs, terminal relaxation of threaded RP chains cannot be achieved by reptation as there are no chain ends in RP. Therefore, a threaded RP chain can only relax by the reptation of the LP chains that thread it, which is referred to as the constraint release (CR) Rouse relaxation mechanism [31–33]. These facts emphasize the importance of threading in determining the rheological properties of the LRB systems. However, a fundamental question that remains to be answered is: what is the relationship between threads and entanglements? As mentioned above, although the CR effect has been thoroughly studied in binary LP blends [34], an exact expression of the relaxation modulus of LRB melts remains unresolved when the threading is considered [34,35]. The threaded RP chain is believed to be relaxed through the CR-Rouse mechanism, the underlying assumption is that the number of LP chains threading RP chain (denoted as the threading number N_T of the RP chain) is considered as the number of entanglements. If it is true, how can we get the value of N_T ? Can it be estimated in advance? In the meantime, what is the exact distribution of N_T ? Note that threading events in LRB are strongly dependent on both the chain length and the composition of the two components [27], then how LP

* Corresponding author. Shenzhen Institute of Advanced Technology, Chinese Academy of Sciences, Shenzhen, 518055, China.

E-mail address: jibao.lu@siat.ac.cn (J. Lu).

<https://doi.org/10.1016/j.polymer.2023.126513>

Received 21 September 2023; Received in revised form 15 November 2023; Accepted 15 November 2023

Available online 24 November 2023

0032-3861/© 2023 Elsevier Ltd. All rights reserved.

component affect the value of N_T ? In this paper, we focus on the LP-dominated LRB system with a fixed composition ($\varphi_L = 0.8$) and try to answer these questions, at least in part.

The polymorphism of RP chains in LRB has been confirmed using the primitive path analysis (PPA) method [27], but it cannot provide the value of N_T *in situ* as well as its distribution. Recently, Hagita et al. have proposed a series of works on the threading statistics of RP chains using the Kremer-Grest (KG) model [36–38]. In their work, N_T is obtained by calculating the Gauss linking number. And to do this, the two ends of the LP chains must be connected by an external chain so that the whole LP chain forms a closed loop. They have successfully calculated the value of N_T and the relationship between size and shape of RP chains with it. The inner minimal surface (IMS) method has been proposed to study the properties of RP chains since 2016 [39], it is a simpler way to detect the threading state between RP and LP chains. Using the IMS method, the threading dynamics of tadpole-like polymer has been reported [40]. In the current work, we systematically investigate the threading events in LRB using the IMS technique. With the aim of relating N_T to entanglement, systems with different combinations of entanglement numbers are constructed. To verify the universality of our conclusion, LRB systems with different chain stiffness are also considered. Details of our models and methods are given in Section 2. Both static and dynamic properties are investigated based on the threading statistics, and the results are provided in Section 3. Finally, our conclusions are summarized in Section 4.

2. Model and method

2.1. Kremer-Grest model

In this work, the standard Kremer-Grest (KG) model [41] with different angular potentials is applied to both LP and RP chains. In this model the monomers interact via the shifted Lennard-Jones type pair potential (WCA potential):

$$U_{\text{pair}}(r) = \begin{cases} 4\epsilon \left[\left(\frac{\sigma}{r}\right)^{12} - \left(\frac{\sigma}{r}\right)^6 + \frac{1}{4} \right], & r < r_c \\ 0, & r > r_c \end{cases}, \quad (1)$$

in which r is the distance between monomers, ϵ is the interaction strength, σ is the length scale unit, and $r_c = 2^{1/6}\sigma$ is the cutoff length of interaction. For bonded monomers, finite extensible nonlinear elastic (FENE) potential is applied:

$$U_{\text{bond}}(r) = \begin{cases} -0.5kR_0^2 \left[1 - \left(\frac{r}{R_0}\right)^2 \right], & r \leq R_0 \\ \infty, & r > R_0 \end{cases}, \quad (2)$$

Here, $k = 30\epsilon/\sigma$ [2] is the spring constant and $R_0 = 1.5\sigma$ is the maximum bond length, which is set to prevent chain crossing. Polymer chains with different stiffness are studied by adjusting the bending coefficient k_θ of the angular potential:

$$U_{\text{angle}} = k_\theta(1 + \cos \theta_0). \quad (3)$$

In this work, three different stiffness are investigated by adjusting the angular term k_θ , $k_\theta = 0.75\epsilon/\sigma^2$, $1.5\epsilon/\sigma^2$ and $2.0\epsilon/\sigma^2$, and the corresponding entanglement lengths N_e are 45, 28 and 23 respectively, which have been determined from monodisperse LP melts using the PPA method in previous work [42].

We systematically prepared LRB with several entanglement number combinations (details of all systems are summarized in Table 1). Both LP and RP chains are placed in a box under periodic boundary conditions with a bead number density of $0.85\sigma^{-3}$. The entanglement numbers of the RP and LP systems are denoted as Z_R and Z_L , respectively. And the value of Z_R and Z_L with different stiffness are both calculated using the corresponding N_e . Note that the predetermined entanglement number is

Table 1

Summary of simulated systems. (N_L : number of beads per linear chain; N_R : number of beads per ring chain; Z_L : entanglement number per linear chain; Z_R : entanglement number per ring chain; C_L : number of linear chains in LRB; C_R : number of ring chains in LRB; τ_{eq} : the equilibrium time steps; τ_{run} : the data collecting time steps.)

	N_L	N_R	Z_L	Z_R	C_L	C_R	τ_{eq}/τ	τ_{run}/τ
$k_0 = 0.75$	125	250	2.78	5.56	1280	160	2×10^8	2×10^8
	250	250	5.56	5.56	640	160	4×10^8	4×10^8
	500	250	11.1	5.56	320	160	1×10^9	8×10^8
	250	125	5.56	2.78	640	320	2×10^8	4×10^8
	250	500	5.56	11.1	640	80	1×10^9	4×10^8
$k_0 = 1.5$	80	160	2.86	5.71	2000	250	2×10^8	2×10^8
	160	160	5.71	5.71	1000	250	4×10^8	4×10^8
	320	160	11.4	5.71	500	250	1×10^9	8×10^8
	160	80	5.71	2.86	1000	500	2×10^8	4×10^8
	160	320	5.71	11.4	1000	125	1×10^9	4×10^8
$k_0 = 2.0$	64	125	2.78	5.57	2500	320	2×10^8	2×10^8
	125	125	5.57	5.57	1250	320	4×10^8	4×10^8
	250	125	10.87	5.57	625	320	1×10^9	8×10^8
	125	64	5.57	2.78	1250	640	2×10^8	4×10^8
	125	250	5.57	10.87	1250	160	1×10^9	4×10^8

an approximate value, we use the exact value of the entanglement number in the fitting, but we don't make the difference among the three cases with similar entanglement number when simply referring to them (e.g., for the shortest chain length used with three stiffnesses, the entanglement numbers are $80/28 = 2.86$, $64/23 = 2.78$, $125/45 = 2.78$, respectively. While we will always refer to them with the closest integer 3. Similarly, systems of longer chains will be referred to as $Z = 6$ and $Z = 11$ for simplicity.). In the following context, the minimum and maximum values of the entanglement number among the chain with three different stiffness are also used, which are denoted as Z_{min} and Z_{max} separately. (i. e. For the case $Z = 6$, $Z_{\text{min}} = 5.56$, $Z_{\text{max}} = 5.71$.) The fraction of LP is denoted as φ . To ensure that the RPs are fully threaded, $\varphi = M_L/M = M_L/(M_L + M_R) = 0.8$, where M_L and M_R are the number of monomers of LPs and RPs, respectively. $M = 200000$ is the total number of monomers in all LRB systems. The monomer density is 0.85, which is the same as the ‘‘canonical’’ Kremer-Grest model [41,43]. So, the box length is $(200000/0.85)^{1/3} = 61.74$. The number of LP and RP chains are denoted as C_L and C_R , so we have $C_L = M\varphi/N_L$, $C_R = M(1-\varphi)/N_R$, where N_R (N_L) is the number of beads per RP (LP) chain. In the trajectory of our simulation, there are at least 80 RP chains (for $N_R = 500$) in each frame to ensure sufficient statistics.

2.2. Simulation details

The LRB model is built by combining pure LP and RP state melts, and the details can be found in our previous work [44]. The temperature of system $T = 1.0\epsilon/k_B$ (k_B denotes the Boltzmann constant), which is controlled using Langevin thermostat with the friction coefficient set as $0.5(mk_B T)^{1/2}/\sigma$. The velocity Verlet algorithm was used for numerical integration of the Langevin equation with a time step $\Delta t = 0.01\tau$, and the time scale $\tau = \sigma(m/\epsilon)^{1/2}$, where m is the mass of a monomer. This model has been widely used in polymer systems, so it is convenient to compare our results with previous studies [8,9,20,30,44]. All simulations were performed using HOOMD-2.9.1 [45], with NVIDIA GTX-V100 graphic cards for acceleration.

The system is equilibrated in two steps. In the first steps, a ‘‘soft’’ force-capped KG model (fcKG) [46] is introduced to help equilibrate the system more effectively. The fcKG model performs a Rouse like dynamics, which could lead to an equilibrium state of the KG melt with a minimum of computational effort. At this stage, we run the simulation using the fcKG model for 10^7 timesteps (more than $2 \times 10^4\tau_e$ for all systems, where τ_e is the entanglement time), and then switch back to the normal KG model. Note that the new force-capped pair potential and the corresponding bonded potential are only applied on LP chains, while the

RP chains interact with the conventional KG model, so that concatenated RP chains are avoided. In the second step, we run the simulation with conventional KG model for a relatively large time steps τ_{eq} (See Table 1) with the aim of obtaining a full equilibrated state of the KG system. For LRB with Z_L or Z_R not exceeding 11, production runs were performed after equilibration runs with 4×10^8 MD steps. While for LRB systems with Z_L or $Z_R = 11$, the equilibration steps are increased to 1×10^9 MD steps. To estimate the properties, snapshots of the system are taken every 10^5 timesteps, so polymer chains in over 2000 frames are averaged in our analysis. Since the total number of monomers are fixed, there are fewer number of RP chains in LRB with longer chain length, so more frames are used (i.e., for systems with Z_L or $Z_R = 11$, the number of frames used is 8000).

2.3. Methods for counting the threads

In order to obtain the exact value of N_T of an RP chain, we should first construct its IMS. In the current work, the IMS of each RP chain is obtained using SurfaceEvolver 2.7.0 with the protocol developed by Smrek et al. [39,47] The IMS of the RP chain is composed of a series of triangles that evolve from an initial surface spanned on the RP chain under surface tension by moving the free vertices (See Fig. 1). Once the IMS has been constructed, the penetration of RP by the LPs can be determined by detecting the relative position of the bonds in the LP chain and the IMS triangles (this is done using Plücker coordinates and the side operator. [39,47]). However, not all penetrations are considered to be effective threading as the chains are highly overlapping at the current monomer number density (0.85). Accordingly, the IMS of an RP chain is always crumpled and twisted, especially as the chain length increases (see Fig. 1). Take the following case as an example: if an LP chain penetrates into the minimal surface of an RP chain twice, then the LP chain is divided into three sub-chains by the point of penetration. If the middle sub-chain is too short (e.g. less than 10 monomers), it cannot be considered an effective thread because this penetration will soon disappear with the change of local configuration. These transient penetrations are common in LRB melts, whereas only those that completely penetrating into the cavity of the RP chains can be considered as effective threads. The detailed protocol for obtaining the effective threading number N_T from the number of penetrations is given in Section S1 of the Supplementary Material. In this paper, we use the subscript R to represent the number of threading LPs per RP chain and L to denote the number of RP chains threaded by LP chains.

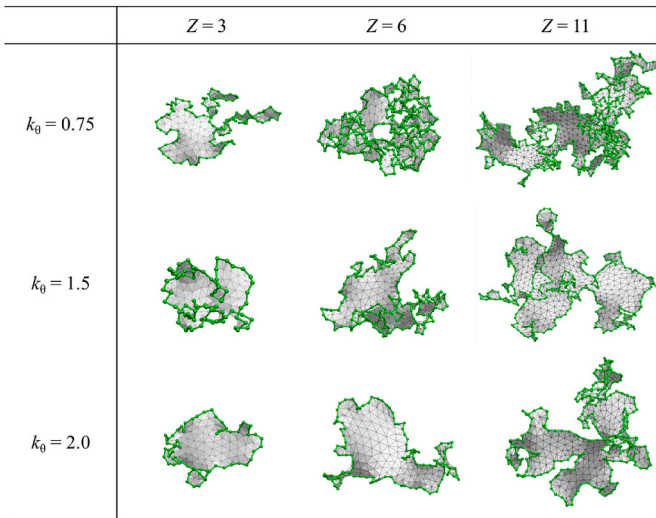


Fig. 1. Snapshots of the IMS of typical RP chains with different stiffness and entanglement number.. (The RP chain configurations are represented by green beads and sticks.)

2.4. Properties

Both static and dynamic properties of polymer chains in LRB are studied. The radius of gyration is used to characterize the size of the polymers, which is calculated as:

$$\langle R_g^2 \rangle = \frac{1}{N} \sum_{i=1}^N (r_i - r_{\text{cm}})^2, \quad (4)$$

in which N is the number of monomers in a single polymer chain, and r_i denotes the position of i th monomer in polymer chain, r_{cm} is the polymer's center of mass. The shape of polymer chain is characterized by the asphericity factor κ , which is obtained from its gyration tensor ($T_{\alpha\beta}$), which is defined using the following equation:

$$\langle T_{\alpha\beta} \rangle = \frac{1}{2N^2} \sum_{i=1}^N \sum_{j=1}^N (r_i^\alpha - r_j^\alpha)(r_i^\beta - r_j^\beta) \quad (5)$$

r_i denotes the α -coordinate of the i th beads, $\alpha, \beta = (x, y, z)$. The value of κ is calculated using the eigenvalues of the gyration tensor with the following equation:

$$\kappa = \frac{(\lambda_1 - \lambda_2)^2 + (\lambda_1 - \lambda_3)^2 + (\lambda_2 - \lambda_3)^2}{2(\lambda_1 + \lambda_2 + \lambda_3)} \quad (6)$$

$\lambda_1, \lambda_2, \lambda_3$ are eigenvalues of $T_{\alpha\beta}$ and $\lambda_1 > \lambda_2 > \lambda_3$, which is obtained through diagonalization of the gyration tensor matrix. κ is a shape factor characterizing the deviation of the polymer chain from a fully spherical shape, and $\kappa \in [0, 1]$. κ is equal to 0 for a spherical shape, 0.25 for a flat disk shape and 1 for a rod-like shape. Meanwhile, we could also obtain the total area (denoted as S) of the IMS for RP chains, which is believed to be another important property characterizing the RP size and shape [39,47]. The results of pure LP and RP melts are also provided for comparison, and these properties of LP/RP chains in the pure state are denoted by the subscript 0. i.e. The square of the radius of gyration for pure RP chain is denoted as $\langle R_g^2 \rangle_{R,0}$.

To represent the dynamics of threading between RP and LP chains, a two-point correlation function is introduced as [40].

$$\chi(t) = \langle T_{ij}(0)T_{ij}(t) \rangle / \langle T_{ij}^2(0) \rangle, \quad (7)$$

in which $T_{ij}(t)$ is the component of the threading matrix of RP with index i and LP with index j at time t . The value of $T_{ij}(t)$ is either 1 or 0. If the i th RP chains are threaded by j th LP chain, then $T_{ij}(t) = 1$, otherwise $T_{ij}(t) = 0$. $\chi(t)$ characterizes the relaxation of threading events, which relates the dynamics of chains to their static properties. Unless otherwise noted, the average of a property X for a polymer chain is denoted as $\langle X \rangle$ in this paper.

3. Results

3.1. Effect of chain length and stiffness on threading numbers

We first focus on systems with fixed entanglement number of LP chains ($Z_L = 6$), where the entanglement number of RP chains varies from 3 to 11. To clarify the relationship between threads and pre-determined entanglements, the N_T values are plotted against the corresponding Z in Fig. 2. We find that the number of threads is close to the number of entanglements determined by PPA methods, since most of the data fall within the range of $Z_R \pm 1$ (indicated by the shaded region in Fig. 2, and the exact value of the deviation is summarized in Table 2). This fact suggests an easy way to estimate the average threading number of RP chains in LP-dominated LRB for a wide range of entanglement numbers ($3 \leq Z_R \leq 11$) (the piercing number is also plotted against the entanglement number of RP chains, and the results and discussion can be found in Section S1 of the Supplementary Material).

It is known that both static and dynamic properties of the RP chain are strongly affected by threading, but they may not be determined by

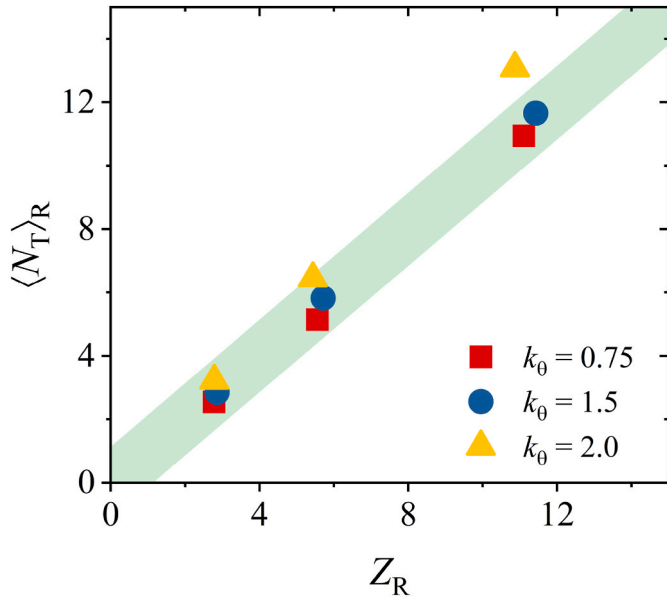


Fig. 2. The average threading number $\langle N_T \rangle$ for RP chains versus the entanglement number of RP chains Z_R . The shaded region indicates $y = x \pm 1$.

an average value alone [48]. Therefore, statistics on the exact

distribution of N_T is also important, and the results are summarized in Fig. 3. By fitting the data with a normal Gaussian function, we can see that the distribution of N_T can be well described for all systems (Fig. 3 (a), (b) and (c)). The mean value obtained by fitting is denoted as \bar{N}_T , and is also plotted against the entanglement number in Fig. 4(d). Like $\langle N_T \rangle$, \bar{N}_T is also close to the value of the corresponding Z_R . The deviation between the threading number and the entanglement number is also summarized in Table 2. In general, $\langle N_T \rangle$ falls in the range of $Z \pm 1$ for most cases, the average value is obtained either by using direct summation over all RP chains ($\langle N_T \rangle$) or Gaussian fitting parameter \bar{N}_T . We also find the largest deviation occurs for the largest RP with the stiffest chain. This fact indicates that care should always be taken when evaluating the average threading number for longer and stiffer RP chains. The width of the distribution is denoted as σ_T and the values of σ_T are listed in Table 2. We find that σ_T increases monotonically with growing chain length and stiffness. The effect of chain length is more significant, so for RP chains with the same stiffness, there will always be a wider threading number distribution in LP dominated LRB. While for RP chains with the same entanglement number Z_R , the distribution is also slightly wider for stiffer chains.

In previous research, the assumption that threading number equals entanglement number is used as a rule of thumb [27], but now we have proof that it is reliable over a fairly wide range of entanglement numbers in LP-dominated LRB. Since the threading number can be roughly estimated from the entanglement number, predicting of the rheological properties of LRB should be less complicated. However, we should

Table 2

The deviation between $\langle N_T \rangle$ or \bar{N}_T and Z_R , and the width of distribution of N_T .

k_θ	$ \langle N_T \rangle - Z_R $			$ \bar{N}_T - Z_R $			σ_T		
	$Z_R = 3$	$Z_R = 6$	$Z_R = 11$	$Z_R = 3$	$Z_R = 6$	$Z_R = 11$	$Z_R = 3$	$Z_R = 6$	$Z_R = 11$
0.75	0.236	0.419	0.437	0.563	0.771	0.675	3.35	4.65	7.05
1.5	0.017	0.104	0.227	0.391	0.337	0.226	3.59	5.24	7.96
2.0	0.437	1.017	2.215	0.064	0.562	1.584	3.82	5.46	8.50

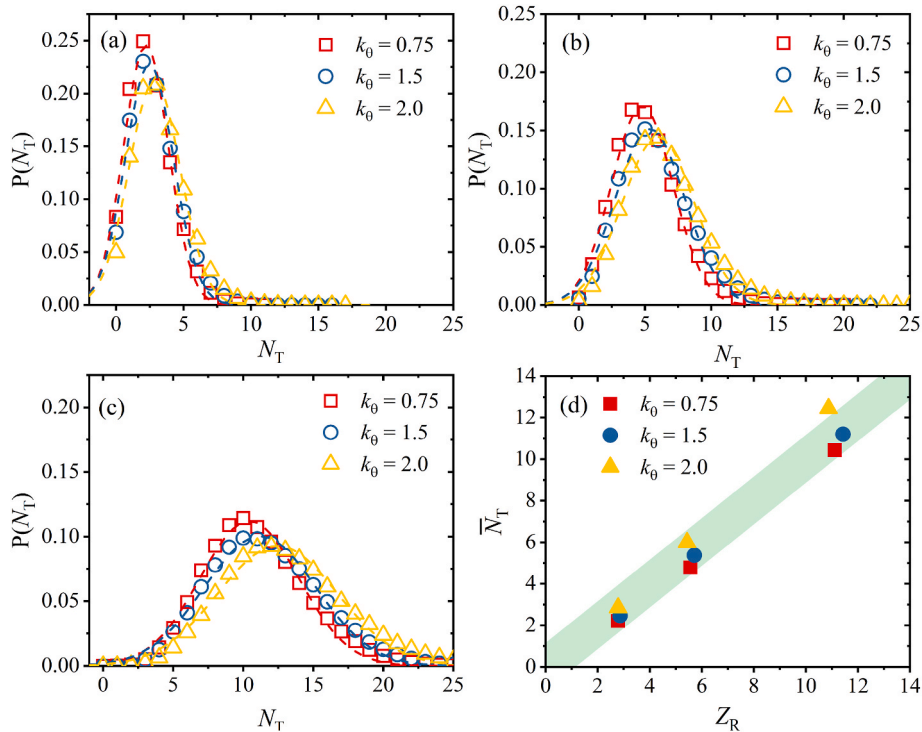


Fig. 3. Probability distribution of the threading number N_T of RP chains in LRB with $Z_L = 6$ and (a) $Z_R = 3$, (b) $Z_R = 6$, (c) $Z_R = 11$. (d) The peak value of the distribution of N_T fitted using normal Gaussian function, the shaded region indicates $y = x \pm 1$.

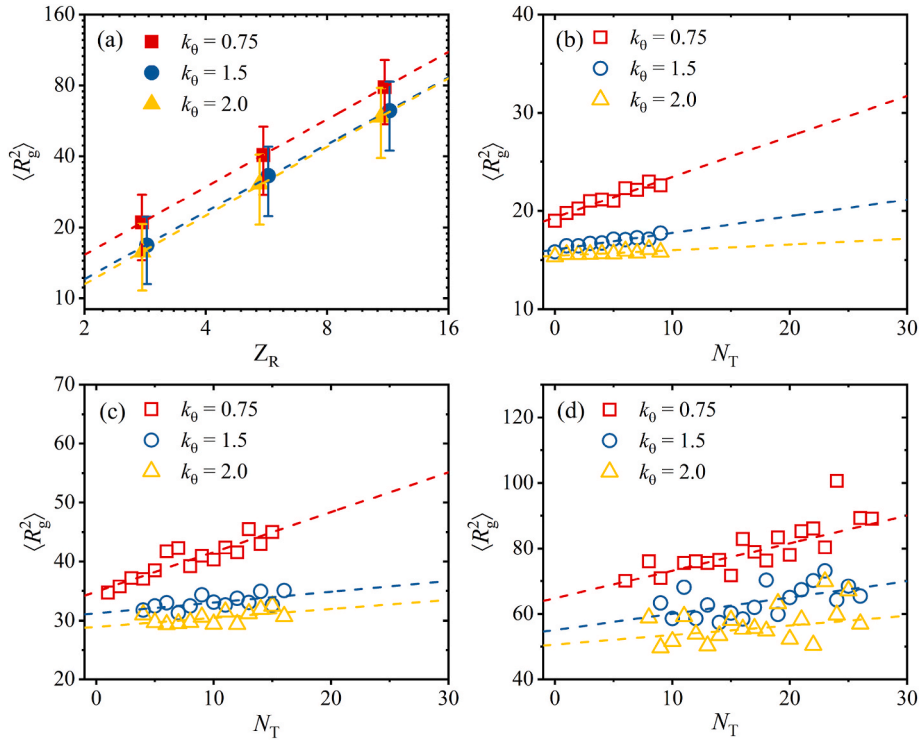


Fig. 4. (a) Dependence of $\langle R_g^2 \rangle$ of Z_R . Dashed lines are fitting curves of the data with $\langle R_g^2 \rangle \sim Z^{a_R}$. Dependence of $\langle R_g^2 \rangle$ on N_T for (b) $Z_R = 3$, (c) $Z_R = 6$, (d) $Z_R = 11$. Dashed lines are linear fitting curves of the data.

always keep in mind that the N_T value close to Z is only an average value, and we do notice that the distribution of N_T is becomes much wider for longer RP chains.

While N_T represents the number of LP chains that threads an RP chain, it is also interesting to check the number of RP chains that an LP chain threads (the average number is denoted as $\langle N_T \rangle_L$) and see if it is influenced by Z_R . On the other hand, we also ask whether $\langle N_T \rangle_R$ is influenced by Z_L . These mutual effects are summarized in section S2 of the Supplementary Material, and we can conclude that there is little dependence of $\langle N_T \rangle_L$ on Z_R and vice versa (Fig. S3).

3.2. Effect of chain length and stiffness on size and shape of RP in LRB

For all systems with $Z_L = 6$, the average value of the radius of gyration for all RPs is plotted against Z_R in Fig. 4(a). For pure RP chains, there should be a relationship $\langle R_g^2 \rangle \sim Z^\nu$, and the scaling factor ν ranges from about 4/5 to 2/3 as chain length increases [3,8,49]. The deviation from ideal chains is attributed to the topological constraints that prevent the expansion of RP chains in the nonconcatenated melt state, where $\langle R_g^2 \rangle \sim Z$. While in LP dominated LRB, RP chains are sufficiently threaded by LP chains. Without the topological constraint, the size of the RP chains should be closer to ideal ones. By fitting the data with a power function, we obtain the scaling exponents ν_R , which are summarized in Table 3. We can see that the value for all stiffness approaches 1.0, indicating that a Gaussian chain like behavior can be expected for RPs in our LRB systems for all stiffness.

Table 3

The scaling factors, together with the slope a_R and a_S .

k_0	ν_R	a_R			ν_S	a_S		
		$Z_R = 3$	$Z_R = 6$	$Z_R = 11$		$Z_R = 3$	$Z_R = 6$	$Z_R = 11$
0.75	0.952	0.413	0.677	0.842	1.141	1.591	2.599	1.599
1.5	0.947	0.169	0.181	0.492	1.146	0.688	1.684	1.235
2.0	0.967	0.058	0.151	0.295	1.165	0.505	1.254	1.735

To investigate the dependence of the threading number on the chain lengths of RPs, the R_g^2 values of RP are averaged for each threading number N_T and plotted in Fig. 4 (b), (c), and (d). It has been reported that the size of RP chains in LP-dominated LRB is linearly proportional with N_T [36,37]. Here in our research, we also find a linear dependence of $\langle R_g^2 \rangle$ on N_T for all cases. However, the fluctuation becomes more significant as N_R increases, which may be due to the poorer statistics for long polymer chains. To compare the sensitivity of RP size with threading number, we fit all the data with linear functions, and the slope a_R are summarized in Table 3. Interestingly, for RP chains with the same chain length, a_R is always larger for more flexible RP chains, indicating that the size of flexible RP chains tends to be more sensitive to threading. This trend is also consistent with the slope value reported by Kasumi et al. In their work, a much larger value around 1.65 is found for a more flexible chain ($k_0 = 0$) [36]. Meanwhile, we also find that a_R monotonically increase with growing Z_R , as shown in Table 3. This indicates that the size of longer RP chains changes more rapidly with increasing N_T .

Similarly, the area of the IMS (which is denoted as S) of RP chains is plotted in Fig. 5. For pure RP chains in nonconcatenated melt state using the same KG model, the scaling factor is about 1.03, while for self-avoiding walk (SAW) chains, the value is 1.176 [39]. By fitting our data, the scaling factors for three stiffnesses are obtained and summarized in Table 3. We can see that for RP chains in LRB, the scaling factor is closer to the predicted value of the SAW chain. If we look at the dependence of S of RP chain on the threading number, a linear

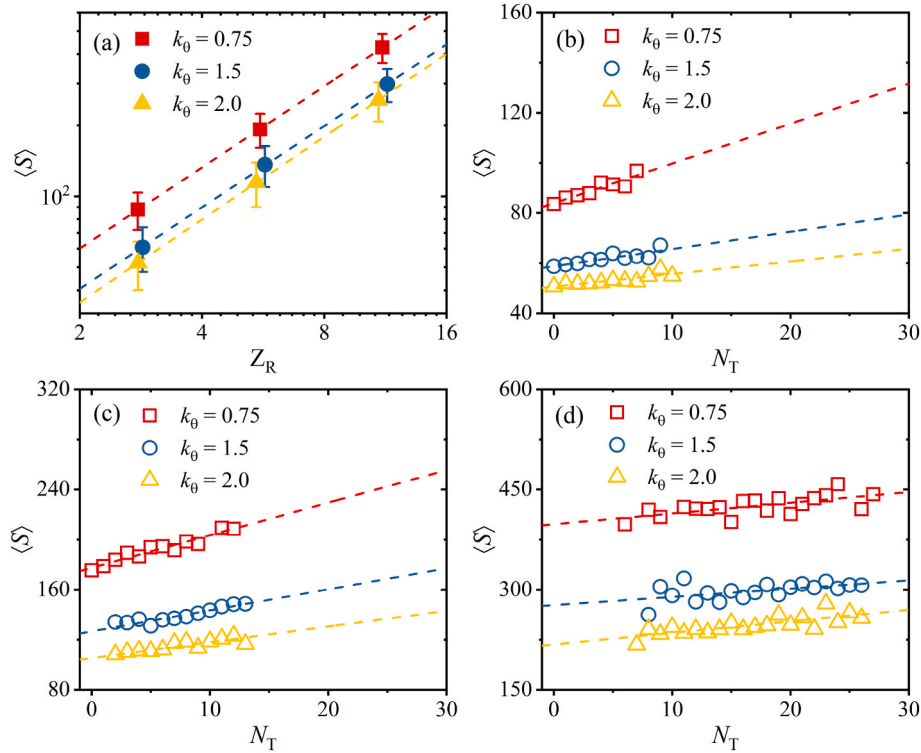


Fig. 5. (a) Dependence of $\langle S \rangle$ with Z_R . Dashed lines are fitting curves with $\langle S \rangle \sim Z^{\alpha_S}$. Dependence of $\langle S \rangle$ on N_T for (b) $Z_R = 3$, (c) $Z_R = 6$, (d) $Z_R = 11$. Dashed lines are linear fitting curves of the data.

relationship is also observed. Again, we fit the data with a linear function and summarize the slope value α_S in Table 3. Consistent with the result of $\langle R_g^2 \rangle$, more flexible RP chains are also found to be more sensitive to threading, as a steeper slope is always found for more flexible chain. While different from R_g^2 , the slope value for S does not increase monotonically with growing chain length. This fact indicates the inner area is not a trivial function of the threading number N_T .

To compare the size of RP chains in LRB and in the pure state, we also calculated the normalized $\langle R_g^2 \rangle$ and $\langle S \rangle$ by dividing these value in pure RP melts (denoted as $\langle R_g^2 \rangle_{R,0}$ and $\langle S \rangle_0$), which is summarized in Table 4. Here we find that the size of RP chains swells more for much longer chains, while the effect of stiffness is tiny, as reflected by the close values in the same column. A similar trend is also found for $\langle S \rangle$ as the chain length increases. While the effect of stiffness is more significant, as we find that the value of normalized $\langle S \rangle$ also increases monotonically with increasing stiffness.

To characterize the shape of RP chains, we calculate the asphericity κ and summarize the results in Fig. 6. From Fig. 6(a), we can see that the difference between RP chains of different stiffness converges to the same value around 0.25 as the chain length increases. Therefore, the difference between RP chains of different stiffness is pronounced for shorter RP chains. While the deviation between RP chains of different stiffness becomes less significant with increasing chain length, that is, the shape of RP chains converges to a uniform shape of a Gaussian ring. In $Z_R = 3$ and $Z_R = 6$ cases, stiffer RP chains with larger κ are found. Therefore, for shorter RP chains in LP dominated LRB, the shape is more extended for

stiffer RP chains. The effect of the threading number on the shape is also investigated. The asphericity for $Z = 3$ case is plotted against N_T in Fig. 6(b), we find that the threading number does not affect the average shape of RP chains, especially for the stiffer chains. For the most flexible case ($k_0 = 0.75$) studied in the current work, the value of κ increase only slightly with N_T , meaning that the shape is not sensitive to threading as much as the size of short RP chain. While as the chain length grows, there is growing trend of increasing value of κ for larger N_T (Fig. 6(c) and (d)), and the value of the κ becomes close to each other for RP chains with different stiffness. While for the largest chain length ($Z = 12$), the increasing trend of κ with N_T is becoming more evident, which means that being threaded by more LP chains, the shape of RP is changing more rapidly from flat (≈ 0.25) to an extended state. However, the effect of stiffness becomes less significant for long RP chains because the data cannot be separated. Meanwhile, the fluctuation of κ is also pronounced, as we have found for the cases of $\langle R_g^2 \rangle$ and $\langle S \rangle$.

The mutual effect between the two types of chains in LRB also needs to be evaluated, i.e., whether the size of the LP chain is changed when mixed with the RP chains of different chain length, and whether the size of RP chain is changed when mixed with LP chains of different chain length. The results are summarized in Section S2 of the Supplementary Material, and we find 20 % RP chain does not induce any change on the size of LP chains. On the other hand, we find a relatively constant swelling ratio (~ 1.30) for RP chains in LRB (Fig. S4 and Table S1 in the Supplementary Material). It means in LP dominated LRB, LP chains can be considered the same as pure LP cases, and RP chains can all be considered as Gaussian rings, regardless of their mixing with shorter or longer LP chains.

Table 4

Summary of the normalized $\langle R_g^2 \rangle$ and $\langle S \rangle$ of RP chains.

k_0	$\frac{\langle R_g^2 \rangle_R}{\langle R_g^2 \rangle_{R,0}}$			$\frac{\langle S \rangle}{\langle S \rangle_0}$		
	$Z_R = 3$	$Z_R = 6$	$Z_R = 11$	$Z_R = 3$	$Z_R = 6$	$Z_R = 11$
0.75	1.190	1.266	1.405	1.140	1.169	1.229
1.5	1.196	1.293	1.409	1.177	1.226	1.274
2.0	1.188	1.297	1.434	1.205	1.259	1.332

3.3. Effect of chain length and stiffness on the dynamics of RP in LRB

As we have discussed above, the effect of threading on RP chains with different chain length and stiffness is revealed by the static properties. To understand how the mutual interplay between LP and RP chains affects their relaxation in LRB, we also determine the dynamics

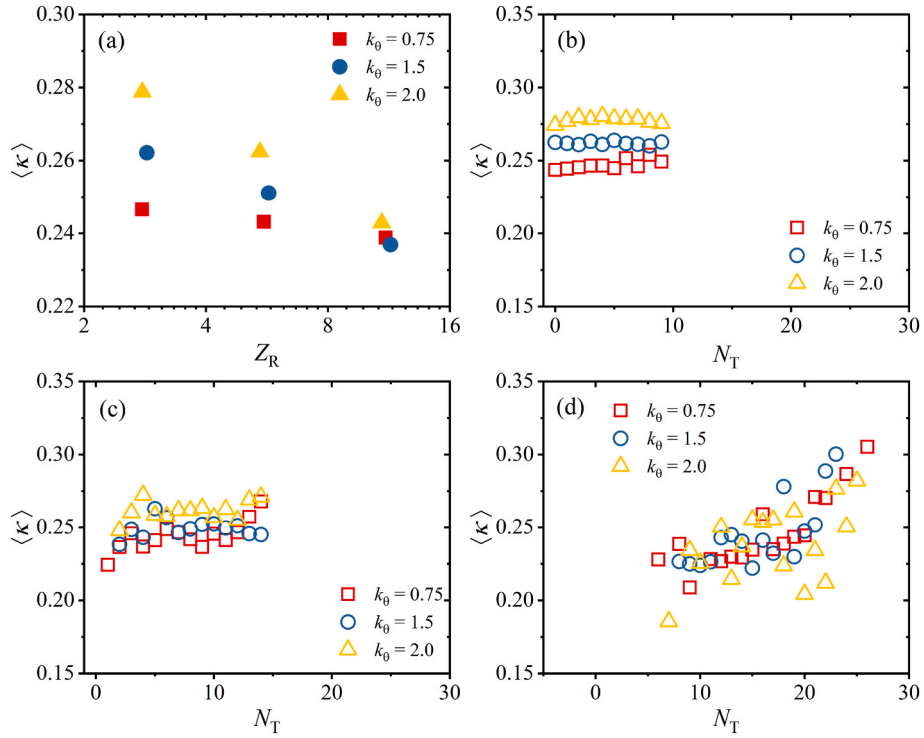


Fig. 6. (a) Averaged asphericity $\langle \kappa \rangle$ versus Z_R . Dependence of $\langle \kappa \rangle$ on N_T for (b) $Z_R = 3$, (c) $Z_R = 6$, (d) $Z_R = 11$.

between RP and LP in LRB systems. In this section, we have summarized the dynamics data of $Z_L = 6$ and $Z_R = 3, 6, 12$, which means that the chain length of LPs is the same in all systems. The dynamics of RP chains are characterized using the two-point correlation function introduced in Section 2.4, and the results are summarized in Fig. 7. For LRB with the same Z_R , we observe that the decay of $\chi(t)$ is much slower for more

flexible chains.

The correlation function can further be fitted using the equation introduced by Rosa et al. [40].

$$\chi(t) = \frac{1}{Z} \int_0^Z \exp[-t / \tau(z)] dz \quad (8)$$

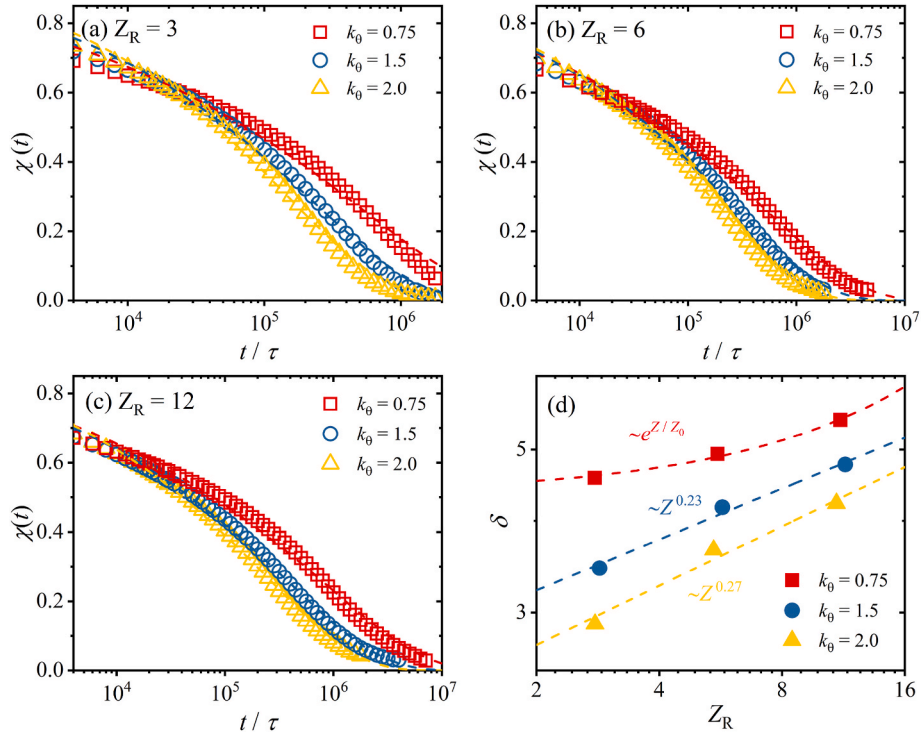


Fig. 7. Two-point correlation function $\chi(t)$ of LRB with $Z_L = 6$ and (a) $Z_R = 3$, (b) $Z_R = 6$ and (c) $Z_R = 12$. Dashed lines are fitting curves using equation (8). (d) The fitting exponential δ for all systems.

In which $\tau(z) = \tau_e z^\delta$, τ_e is the entanglement timescale, and δ is a generic exponent characterizing the dynamics of chain threading. The values of τ_e and δ for different LRB systems can be obtained simultaneously by fitting the correlation function data using equation (8). Here we define a characteristic relaxation time τ_r as the corresponding time when $\chi(t)$ decays from 0.4 to 0.2 (To reduce the systematic error, which is more pronounced for more flexible chains, we use the initial value of 0.4 instead of 1.0. The corresponding values of time t for $\chi(t) = 0.4$ and 0.2 are summarized in Table S2 in the Supplementary Material). The values of τ_r , τ_e and δ are given in Table 5. We found that the relaxation time τ_r monotonically increase with growing Z_R , suggesting that the relaxation is slowed down by pronounced threading. Meanwhile, it is clear that more flexible chains are always found with much longer relaxation times. In the previous section we found that more flexible chains are more sensitive to threads, here we find that it also results in much slower dynamics. The entanglement timescale τ_e decrease with increasing Z_R for all cases, which is reminiscent of the work of Michieletto et al. [40] According to their results, the microscopic timescale values also slightly decrease with increasing tail length of the tadpole-like polymer. Furthermore, we find that δ increases monotonically with increasing Z_R , and for most cases, the value is larger than 3.0, indicating much slower relaxation dynamics than chain reptation [40]. This fact is consistent with the experiment and our recent finding that fully penetrated RP relaxes through a CR-Rouse dynamics. Meanwhile, the most flexible systems are found with the largest δ , and δ increases exponentially. While for much stiffer chains, the value of δ is also smaller, with a power-law relationship of Z_R . This implies that the dynamics of the polymer chain diverges more strongly than an exponential for LRB with more flexible chains [40].

As the average value of N_T can be approximated by the entanglement number for LRB of all stiffnesses, the dynamics are significantly different. More flexible LRBs show much slower dynamics compared to those of stiffer ones, which may be partly due to their systematically larger size (See Figs. 4 and 5). On the other hand, we have found that the threading number is roughly the same for RPs with similar entanglement length but different stiffness (the value for flexible chains is slightly smaller), but a narrower distribution is found for much more flexible cases. This fact indicates that the distribution of threading number plays very important role on the dynamics of RP chains, those with different threading number could behave very differently. Obviously, using an average value is not sufficient to fully describe the rheological properties of LRB. In our study, we find that a wider distribution of threading number the accelerates the dynamics, which is most likely due to the relatively faster relaxation of those RP chains with smaller threading numbers [25,30,50].

4. Conclusion

In this paper, we systematically study LP-dominated LRB systems with different chain length and stiffness by using KG model. The number of threading (N_T) through RPs by LPs are counted with the IMS technique. We then thoroughly investigate the effect of the statistics of N_T on both the static and dynamics of RP chains, with several key conclusions obtained as follows:

- (1) Within a wide range of chain length, the average value of N_T is larger for longer RP chains. For RP chains with different stiffness, N_T can be roughly evaluated by their entanglement number (Z_R).
- (2) N_T follows a Gaussian distribution. The width of the distribution increases with both the chain length and the stiffness of RP chains.
- (3) The size of RP chains and the total area of IMS increase monotonically with growing N_T , and a linear relationship is found for smaller threading number range. The sensitivity to threading is more pronounced for longer and more flexible chains. Similarly, the area of IMS also depends linearly on the threading number. However, the sensitivity is pronounced for more flexible chains, but not for longer chains.
- (4) For the shape of RP chains, as the chain length increases, all RP chains are found to have a uniform shape with $\kappa \approx 0.25$. Moreover, the effect of threading on the shape of the RP is also enhanced for longer chains, but the stiffness is becomes a less significant factor.
- (5) Chain stiffness strongly influences the threading dynamics, as more flexible RP chains show a much longer relaxation time compared to much stiffer ones. This may be partly due to the relatively larger size of flexible RP chains, and we believe that the distribution of threading number also plays an important role.

Besides the main conclusions above, we find that, in LP dominated LRB, the entanglement number of LP is only related to the chain length of the LP itself, regardless of the RP counterpart; the threading number of RP is not related to the chain length of its LP counterpart either, which applies to all the systems with the three stiffnesses. It implies that in LP-dominated LRB, the number of threads of RP (or the number of entanglements of LP), which is a key parameter in the rheological properties of LRB, could be predetermined independently of the chain length of the other component.

Note that only one composition is discussed in this work ($\phi_L = 0.8$); study on other LP/RP ratio is also underway to provide a complete picture of the LRB system. The exact distribution of threading is required to obtain a more accurate estimate of the relaxation modulus of LRB, which is an important rheological issue to be studied in the future. Moreover, LRB systems with both more flexible ($k_0 < 0.75\epsilon/\sigma$ [2]) and stiffer ($k_0 > 2.0\epsilon/\sigma$ [2]) chains are also important for the completeness of the discussion. Simulations and evaluations of the rheological properties of LRB both in equilibrated state and under shear/elongational flow are also in progress and the results will be reported in subsequent work.

CRedit authorship contribution statement

Wei Wang: Writing – original draft, Conceptualization, Methodology, Data curation. **Jibao Lu:** Supervision, Resources, Writing – review & editing. **Rong Sun:** Resources.

Declaration of competing interest

The authors declare that they have no known competing financial interests or personal relationships that could have appeared to influence the work reported in this paper.

Table 5
Summary of the characteristic time τ_r , τ_e and δ

k_0	$\tau_r/10^5\tau$			$\tau_e/10^3\tau$			δ		
	$Z_R = 3$	$Z_R = 6$	$Z_R = 11$	$Z_R = 3$	$Z_R = 6$	$Z_R = 11$	$Z_R = 3$	$Z_R = 6$	$Z_R = 11$
0.75	7.61	8.05	12.1	1.61	0.376	0.143	4.58	5.28	5.48
1.5	3.87	4.26	5.57	3.66	0.965	0.219	3.45	4.17	4.77
2.0	2.66	3.01	3.89	5.27	1.47	0.376	2.89	3.65	4.23

Data availability

Data will be made available on request.

Acknowledgement

This work was supported by the National Natural Science Foundation of China (no. 52003289), the Youth Innovation Promotion Association CAS (no. 2021363), the top-notch Young Talents of Science and Technology Innovation of Guangdong Special Support Program (no. 2021TQ06C108) and Guangdong Basic and Applied Basic Research Foundation. (no. 2023A1515011167).

Appendix A. Supplementary data

Supplementary data to this article can be found online at <https://doi.org/10.1016/j.polymer.2023.126513>.

References

- J. des Cloizeaux, M.L. Mehta, Topological constraints on polymer rings and critical indices, *J. Phys.* 40 (7) (1979) 665–670.
- J. des Cloizeaux, Ring polymers in solution : topological effects, *J. Phys., Lett.* 42 (19) (1981) 433–436.
- M.E. Cates, J.M. Deutsch, Conjectures on the statistics of ring polymers, *J. Phys.* 47 (12) (1986) 2121–2128.
- S.P. Obukhov, M. Rubinstein, T. Duke, Dynamics of a ring polymer in a gel, *Phys. Rev. Lett.* 73 (9) (1994) 1263–1266.
- M. Muller, J.P. Wittmer, M.E. Cates, Topological effects in ring polymers: a computer simulation study, *Phys. Rev.* 53 (5) (1996) 5063–5074.
- M. Muller, J.P. Wittmer, M.E. Cates, Topological effects in ring polymers. II. Influence of persistence length, *Phys. Rev.* 61 (4) (2000) 4078–4089.
- S.T. Milner, J.D. Newhall, Stress relaxation in entangled melts of unlinked ring polymers, *Phys. Rev. Lett.* 105 (20) (2010), 208302.
- J.D. Halverson, W.B. Lee, G.S. Grest, A.Y. Grosberg, K. Kremer, Molecular dynamics simulation study of nonconcatenated ring polymers in a melt. I. Statics, *J. Chem. Phys.* 134 (20) (2011), 204904.
- J.D. Halverson, W.B. Lee, G.S. Grest, A.Y. Grosberg, K. Kremer, Molecular dynamics simulation study of nonconcatenated ring polymers in a melt. II. Dynamics, *J. Chem. Phys.* 134 (20) (2011), 204905.
- T. Sakaue, Statistics and geometrical picture of ring polymer melts and solutions, *Phys. Rev. E – Stat. Nonlinear Soft Matter Phys.* 85 (2 Pt 1) (2012), 021806.
- J. Suzuki, A. Takano, Y. Matsushita, Chain conformations of ring polymers under theta conditions studied by Monte Carlo simulation, *J. Chem. Phys.* 139 (18) (2013), 184904.
- S. Goossen, A.R. Bras, M. Krutyeva, M. Sharp, P. Falus, A. Feoktystov, U. Gasser, W. Pyckhout-Hintzen, A. Wischniewski, D. Richter, Molecular scale dynamics of large ring polymers, *Phys. Rev. Lett.* 113 (16) (2014), 168302.
- S. Obukhov, A. Johner, J. Baschnagel, H. Meyer, J.P. Wittmer, Melt of polymer rings: the decorated loop model, *EPL* 105 (4) (2014), 48005.
- A.Y. Grosberg, Annealed lattice animal model and Flory theory for the melt of nonconcatenated rings: towards the physics of crumpling, *Soft Matter* 10 (4) (2014) 560–565.
- Y. Doi, K. Matsubara, Y. Ohta, T. Nakano, D. Kawaguchi, Y. Takahashi, A. Takano, Y. Matsushita, Melt rheology of ring polystyrenes with ultrahigh purity, *Macromolecules* 48 (9) (2015) 3140–3147.
- Z.-C. Yan, S. Costanzo, Y. Jeong, T. Chang, D. Vlassopoulos, Linear and nonlinear shear rheology of a marginally entangled ring polymer, *Macromolecules* 49 (4) (2016) 1444–1453.
- J. Qin, S.T. Milner, Tube dynamics works for randomly entangled rings, *Phys. Rev. Lett.* 116 (6) (2016), 068307.
- T. Ge, S. Panyukov, M. Rubinstein, Self-similar conformations and dynamics in entangled melts and solutions of nonconcatenated ring polymers, *Macromolecules* 49 (2) (2016) 708–722.
- D. Michieletto, On the tree-like structure of rings in dense solutions, *Soft Matter* 12 (47) (2016) 9485–9500.
- T. Ge, J.T. Kalathi, J.D. Halverson, G.S. Grest, M. Rubinstein, Nanoparticle motion in entangled melts of linear and nonconcatenated ring polymers, *Macromolecules* 50 (4) (2017) 1749–1754.
- V. Arrighi, J.S. Higgins, Local effects of ring topology observed in polymer conformation and dynamics by neutron scattering-A review, *Polymers* 12 (9) (2020).
- Y. Ederle, K.S. Naraghi, P.J. Lutz, Synthesis of cyclic macromolecules, in: *Synthesis of Polymers*, 1998, pp. 621–647.
- G. Tsolou, N. Stratikis, C. Baig, P.S. Stephanou, V.G. Mavrantzas, Melt structure and dynamics of unentangled polyethylene rings: Rouse theory, atomistic molecular dynamics simulation, and comparison with the linear analogues, *Macromolecules* 43 (24) (2010) 10692–10713.
- W. Wang, C.S. Biswas, C.C. Huang, H. Zhang, C.Y. Liu, F.J. Stadler, B. Du, Z.C. Yan, Topological effect on effective local concentration and dynamics in linear/linear, ring/ring, and linear/ring miscible polymer blends, *Macromolecules* 53 (2) (2020) 658–668.
- S. Nam, J. Leisen, V. Breedveld, H.W. Beckham, Melt dynamics of blended poly (oxyethylene) chains and rings, *Macromolecules* 42 (8) (2009) 3121–3128.
- G.D. Papadopoulos, D.G. Tsaliakis, V.G. Mavrantzas, Microscopic dynamics and topology of polymer rings immersed in a host matrix of longer linear polymers: results from a detailed molecular dynamics simulation study and comparison with experimental data, *Polymers* 8 (8) (2016) 21.
- D.G. Tsaliakis, V.G. Mavrantzas, Threading of ring poly(ethylene oxide) molecules by linear chains in the melt, *ACS Macro Lett.* 3 (8) (2014) 763–766.
- S. Goossen, A.R. Bras, W. Pyckhout-Hintzen, A. Wischniewski, D. Richter, M. Rubinstein, J. Roovers, P.J. Lutz, Y. Jeong, T. Chang, D. Vlassopoulos, Influence of the solvent quality on ring polymer dimensions, *Macromolecules* 48 (5) (2015) 1598–1605.
- M. Kapnistos, M. Lang, D. Vlassopoulos, W. Pyckhout-Hintzen, D. Richter, D. Cho, T. Chang, M. Rubinstein, Unexpected power-law stress relaxation of entangled ring polymers, *Nat. Mater.* 7 (12) (2008) 997–1002.
- J.D. Halverson, G.S. Grest, A.Y. Grosberg, K. Kremer, Rheology of ring polymer melts: from linear contaminants to ring-linear blends, *Phys. Rev. Lett.* 108 (3) (2012), 038301.
- M.J. Struglinski, W.W. Graessley, Effects of polydispersity on the linear viscoelastic properties of entangled polymers. 1. EXPERIMENTAL-OBSERVATIONS for binary-mixtures of linear polybutadiene, *Macromolecules* 18 (12) (1985) 2630–2643.
- J.L. Viovy, M. Rubinstein, R.H. Colby, Constraint release in polymer melts – tube reorganization versus tube dilation, *Macromolecules* 24 (12) (1991) 3587–3596.
- D.J. Read, M.E. Shvokhin, A.E. Likhtman, Contour length fluctuations and constraint release in entangled polymers: slip-spring simulations and their implications for binary blend rheology, *J. Rheol.* 62 (4) (2018) 1017–1036.
- Z.W. Wang, R.G. Larson, Constraint release in entangled binary blends of linear polymers: a molecular dynamics study, *Macromolecules* 41 (13) (2008) 4945–4960.
- D. Parisi, J. Ahn, T. Chang, D. Vlassopoulos, M. Rubinstein, Stress relaxation in symmetric ring-linear polymer blends at low ring fractions, *Macromolecules* 53 (5) (2020) 1685–1693.
- K. Hagita, T. Murashima, Effect of chain-penetration on ring shape for mixtures of rings and linear polymers, *Polymer* 218 (2021).
- K. Hagita, T. Murashima, Molecular dynamics simulations of ring shapes on a ring fraction in ring-linear polymer blends, *Macromolecules* 54 (17) (2021) 8043–8051.
- K. Hagita, T. Murashima, Multi-ring configurations and penetration of linear chains into rings on bonded ring systems and polycatenanes in linear chain matrices, *Polymer* 223 (2021).
- J. Smrek, A.Y. Grosberg, Minimal surfaces on unconcatenated polymer rings in melt, *ACS Macro Lett.* 5 (6) (2016) 750–754.
- A. Rosa, J. Smrek, M.S. Turner, D. Michieletto, Threading-induced dynamical transition in tadpole-shaped polymers, *ACS Macro Lett.* 9 (5) (2020) 743–748.
- K. Kremer, G.S. Grest, Dynamics of entangled linear polymer melts: a molecular-dynamics simulation, *J. Chem. Phys.* 92 (8) (1990) 5057–5086.
- R. Everaers, S.K. Sukumaran, G.S. Grest, C. Svaneborg, A. Sivasubramanian, K. Kremer, Rheology and microscopic topology of entangled polymeric liquids, *Science* 303 (5659) (2004) 823–826.
- R. Everaers, H.A. Karimi-Varzaneh, F. Fleck, N. Hojdis, C. Svaneborg, Kremer–grest models for commodity polymer melts: linking theory, experiment, and simulation at the kuhn scale, *Macromolecules* 53 (6) (2020) 1901–1916.
- W. Wang, C.S. Biswas, C. Huang, H. Zhang, C.-Y. Liu, F.J. Stadler, B. Du, Z.-C. Yan, Topological effect on effective local concentration and dynamics in linear/linear, ring/ring, and linear/ring miscible polymer blends, *Macromolecules* 53 (2) (2020) 658–668.
- J.A. Anderson, C.D. Lorenz, A. Travesset, General purpose molecular dynamics simulations fully implemented on graphics processing units, *J. Comput. Phys.* 227 (10) (2008) 5342–5359.
- C. Svaneborg, H.A. Karimi-Varzaneh, N. Hojdis, F. Fleck, R. Everaers, Multiscale approach to equilibrating model polymer melts, *Phys. Rev. E* 94 (3–1) (2016), 032502.
- J. Smrek, K. Kremer, A. Rosa, Threading of unconcatenated ring polymers at high concentrations: double-folded vs time-equilibrated structures, *ACS Macro Lett.* 8 (2) (2019) 155–160.
- T. Vettorel, K. Kremer, Development of entanglements in a fully disentangled polymer melt, *Macromol. Theory Simul.* 19 (1) (2010) 44–56.
- T. Sakaue, Ring polymers in melts and solutions: scaling and crossover, *Phys. Rev. Lett.* 106 (16) (2011), 167802.
- J. Klein, Dynamics of entangled linear, branched, and cyclic polymers, *Macromolecules* 19 (1) (1986) 14.